MgII and CIV absorbers along GRB lines of sight

S.D. Vergani, P. Petitjean, C. Ledoux, P. Vreeswijk, A. Smette

The study of Gamma Ray Burst (GRB) lines of sight (los) has been boosted thanks to very rapid high resolution observations of GRB afterglow spectra. The spectra allow a detailed analysis of the absorbers seen at all redshifts. In the last few years there has been a growing interest in the comparison of these absorbers with QSO absorption line systems. In particular, Prochter et al. (2006b, ApJL 648, 93) found that the incidence of strong MgII intervening systems (rest equivalent width Wr > 1Å) along GRB sight lines is ~ 4 times higher (number density dN/dz = 0.90 ± 0.24) than what is seen in the SDSS along QSO lines of sight. Sudilovski et al. (2008, ApJ 669, 741) confirmed this result on the basis of UVES observations.

We analyse 9 GRB lines of sight all observed with VLT-UVES @ ESO concentrating on both WEAK and STRONG MgII absorbers. For each line of sight we search for both the weak and strong MgII absorbers outside the Ly-α forest. We consider MgII components within 500 km/s as a single systems. Tab. 1 and Fig. 1 summarize our results.
Prochter et al. (2006b) set for their analysis a redshift range 0.359-2 to compare the results to those of the SDSS on QSOs reported by Prochter et al. (2006a, ApJ 639, 766) (even if the z_{end} in this case was 2.3). If the MgII doublet wavelength is inside the spectral range, they set the ending redshift as the one corresponding to a velocity ejection of 3000 km/s1 from the GRB. This condition is usually set also for QSO survey studies to try to avoid the inclusion in the sample of MgII absorbers local to the QSO.
Since we are considering also weak systems, we compare our results to the Nestor et al. (2005, ApJ 628, 637) work on the SDSS QSO lines of sight. They have limits at z_{start}=0.366 and z_{end}=2.27. Tab. 2 reports the number of systems we find (also considering the redshift ranges used by Prochter et al. 2006b or Nestor et al. 2005) for Wr < 0.3 Å, 0.3 ≤ Wr ≤ 1 Å and Wr > 1 Å, compared to those predicted using the results on QSO los of Prochter et al. (2006a) and Nestor et al. (2005).

Table 1: MgII absorbers

GRB	z_{GRB}	$dz_{W>0.3}$	$dz_{W>1}$	z_{abs}	$W_r(2796$ Å)	Δv_{abs} (km/s)	Δv_{ej} (km/s)	Remarks
021004	2.3295	1.675	1.787	0.5550	0.248 ± 0.025	~ 40	~ 192000	blended with $AlII_{1670}$ at $z = 1.60262$
				1.3800	1.637 ± 0.020	~ 280	~ 97000	
				1.6026	1.407 ± 0.024	~ 250	~ 72000	
				1.7809	0.078 ± 0.019	~ 15	~ 53000	
050730	3.9687	0.718	1.243	1.7732	0.927 ± 0.030	~ 130	~ 157000	
				2.2531	< 0.783 (0.650)	~ 140	~ 120000	sky contamination (subtracted)
050820	2.6147	1.655	1.845	0.6896	0.089 ± 0.007	~ 30	~ 192000	
				0.6915	2.874 ± 0.007	~ 470	~ 192000	
				1.4288	1.323 ± 0.023	~ 345	~ 113000	
				1.6204	0.277 ± 0.024	~ 85	~ 93000	
				2.3598	< 0.424 (0.306)	~ 60	~ 22000	bad S/N and blending with GRB $FeII_{2600}$ (subtracted)
050922C	2.1991	1.554	1.701	0.6369	0.179 ± 0.018	~ 60	~ 175000	
				1.1076	0.677 ± 0.029	~ 185	~ 118000	
				1.5970	< 0.102 (0.08)	~ 40	~ 62000	sky contamination (subtracted)
				2.0778	> 1 Å	?	~ 12000	not covered because of spectrum cut
060418	1.4900	1.242	1.265	0.6026	1.293 ± 0.010	~ 260	~ 124000	
				0.6559	1.033 ± 0.006	~ 345	~ 116000	
				1.1070	1.844 ± 0.014	~ 315	~ 50000	
060607A	3.0748	1.529	1.660	1.5103	0.204 ± 0.011	~ 190	~ 135000	
				1.8033	1.854 ± 0.006	~ 390	~ 107000	
				2.2783	0.343 ± 0.058	~ 60	~ 64000	
071031	2.6922	1.509	1.789	1.0743	0.330 ± 0.016	~ 145	~ 156000	
				1.6419	0.692 ± 0.014	~ 160	~ 97000	
				1.9520	0.884 ± 0.016	~ 300	~ 66000	
080310	2.4272	1.786	1.841	1.1788	0.047 ± 0.024	~ 30	~ 127000	
				1.6711	0.421 ± 0.012	~ 95	~ 73000	
				2.0685	?	?	~ 33000	not covered because of spectrum cut
080319B	0.9378	0.790	0.790	0.5308	0.614 ± 0.001	~ 110	~ 69000	
				0.5662	0.083 ± 0.003	~ 30	~ 63000	
				0.7154	1.482 ± 0.001	~ 420	~ 36000	
				0.7608	0.108 ± 0.002	~ 100	~ 29000	

Tab. 1 : Detected MgII systems. The redshift paths are computed for the 2 different Wr lower limits (0.3 and 1 Å) . Δv_{abs} is the velocity spread by each absorber. Δv_{ej} is the ejection velocity relative to the GRB.

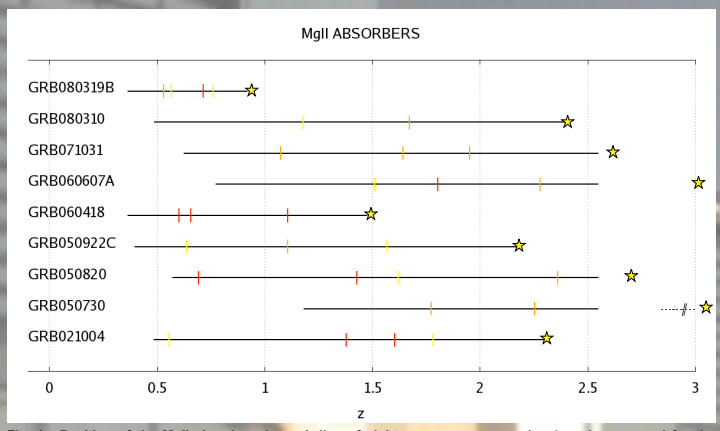

Fig. 1 : Position of the MgII absorbers in each line of sight. Yellow, orange and red marks are used for the systems with Wr < 0.3 Å, 0.3 ≤ Wr ≤ 1 Å and Wr > 1 Å, respectively. The black horizontal solid lines represent the MgII redshift range. The positions of GRBs are shown as stars.

	$N(W_r > 0.3)$ Å	$N(0.3 \leq W_r \leq 1$ Å)	$N(W_r > 1$ Å)
GRBs (this study, $0.366 < z < 2.27$)	17	8	9
GRBs (this study, $0.359 < z < 2$)	16	7	9
GRBs (Prochter et al. 2006b)			14
QSOs (Nestor et al. 2005)	8.9	5.7	
QSOs (Prochter et al. 2006a)			2

Tab. 2 : Number of MgII system found in our sample compared to the predicted number obtained using the results of Nestor et al. (2005) and Prochter et al. (2006a) on QSO los.

Compared to the results of Nestor et al. (2005), the total number of MgII systems is a factor of ~2 larger, while the number of systems with 0.3 ≤ Wr ≤ 1 Å is CONSISTENT.

We confirm the excess of STRONG MgII systems along GRB los

DUST BIAS in QSOs

One possibility to explain the difference could be that we do not observe QSO lines of sight with several strong MgII sytems because of dust attenuation. If true we should see an excess of extinction in GRBs.

Measurements of dust depletion and extinction in 4 of the 9 strong MgII systems of the sample are reported in Table 3. For the remaining 5 systems suitable absorption lines are not in the spectral range. We find visual attenuation consistent with what is seen in QSOs. Even if in 2 cases there is evidence of relatively strong dust depletion ([Fe/Zn]=-1), the low metal column density (log N(ZnII)< 13) implies a low amount of extinction.

These results DO NOT FAVOUR the DUST BIAS as an explanation of the excess of strong MgII absorbers.

	z	[Fe/Zn]	[Fe/Si]	A_V
GRB021004	1.3800		-0.05	0
GRB021004	1.6026	-1.03		< 0.3
GRB060418	1.1070	-1.05		< 0.3
GRB060607A	1.8033		-0.24	0

Tab. 3 : Table reporting the iron to zinc or iron to silicon ratio and the inferred visual attenuation caused by the strong MgII systems present along the line of sight of GRB021004, GRB060607A and the z=1.1070 system along the GRB060418 line of sight.

EJECTED SYSTEMS

It is possible that some of the strong MgII absorbers are due to ejected material local to the GRBs and endowed with large proper motion.

We will test this hypothesis looking at the distribution of CIV absorbers. These systems are expected to trace better ejected material.
The position of the systems along the lines of sight are shown in Figure 2 and summarized in Table 4.

In all cases except GRB071031 there is AT LEAST 1 ABSORBER inside a velocity range of about 5000km/s from the GRB.

We also find a hint for enhanced CLUSTERING of CIV absorbers in the vicinity of the GRB (but further investigation is needed).

GRB	z_{GRB}	z_{abs}	Δv_{ej}(km/s)
021004	2.3295	2.2970	~ 2000
		2.3219	~ 700
050730	3.9687	3.5142	~ 29000
		3.5640	~ 25000
		3.5990	~ 24000
		3.9445	~ 1500
050820	2.6147	2.0748	~ 48000
		2.1463	~ 41000
		2.3238	~ 25000
		2.3598	~ 22000
		2.5706	~ 4000
050922C	2.1991	1.5693	~ 62000
		1.9891	~ 20000
		2.0086	~ 18000
		2.0778	~ 12000
		2.1421	~ 5000
060607A	3.0748	2.2165	~ 70000
		2.2783	~ 64000
		2.3114	~ 62000
		2.8700	~ 16000
		2.8822	~ 15000
		2.8896	~ 14000
		2.8972	~ 14000
		2.9166	~ 12000
		2.9295	~ 11000
		2.9373	~ 11000
		3.0498	~ 2000
071031	2.6922	1.9520	~ 66000
		2.3749	~ 27000
080310	2.4272	2.0685	~ 33000
		2.1702	~ 23000
		2.2786	~ 13000
		2.3400	~ 8000
		2.4112	~ 1400
		2.4199	~ 600

Tab. 4 : CIV absorber redshifts, z_{abs}, and corresponding ejection velocity Δv_{ej}

LENSING

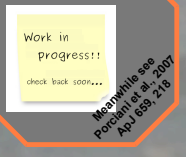

Meanwhile see Porciani et al., 2007 ApJ 659, 218

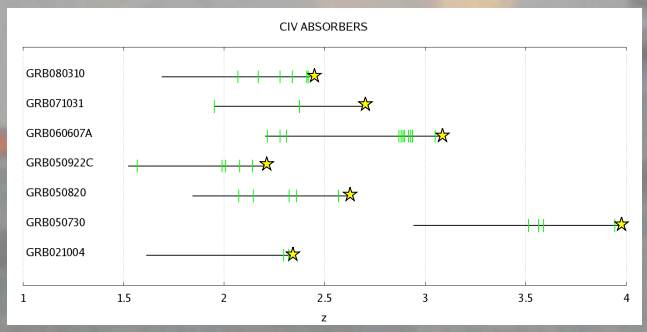

Fig. 2 : The position of CIV absorbers are represented with green marks. The black horizontal lines represent the CIV redshift range covered by the UVES spectra. The positions of GRBs are shown as stars.

Picture by Y. Bresson